Biophysical Journal Volume 100 April 2011 2024–2032

Naproxen Interferes with the Assembly of Aβ Oligomers Implicated in Alzheimer's Disease

Seongwon Kim,[†] Wenling E. Chang,[†‡] Rashmi Kumar,[†] and Dmitri K. Klimov[†*]
[†]School of Systems Biology, George Mason University, Manassas, Virginia; and [‡]The MITRE Corporation, San Diego, California

ABSTRACT Experimental and epidemiological studies have shown that the nonsteroidal antiinflammatory drug naproxen may be useful in the treatment of Alzheimer's disease. To investigate the interactions of naproxen with Aβ dimers, which are the smallest cytotoxic aggregated Aβ peptide species, we use united atom implicit solvent model and exhaustive replica exchange molecular dynamics. We show that naproxen ligands bind to Aβ dimer and penetrate its volume interfering with the interpeptide interactions. As a result naproxen induces a destabilizing effect on Aβ dimer. By comparing the free-energy landscapes of naproxen interactions with Aβ dimers and fibrils, we conclude that this ligand has stronger antiaggregation potential against Aβ fibrils rather than against dimers. The analysis of naproxen binding energetics shows that the location of ligand binding sites in Aβ dimer is dictated by the Aβ amino acid sequence. Comparison of the in silico findings with experimental observations reveals potential limitations of naproxen as an effective therapeutic agent in the treatment of Alzheimer's disease.

INTRODUCTION

A number of age-related disorders, including Alzheimer's, Parkinson's, and Creutzfeldt-Jakob diseases, are associated with aberrant aggregation of polypeptide chains and formation of amyloid fibrils (1,2). Biomedical experiments and genetic studies suggested that the onset of Alzheimer's disease (AD) is related to aggregation of Aβ peptides (3), which are derived from the transmembrane amyloid precursor protein in the course of proteolysis. Although these peptides have varying lengths, the 40-residue species, $A\beta_{1-40}$, are most abundant. Their assembly into amyloid fibrils involves multiple conformational transitions, in which oligomeric species appear as intermediates (2,4,5). It is well known that Aβ fibrils are cytotoxic (6), but recent findings pointed to Aβ oligomers as primary cytotoxic species in AD (7–9). Furthermore, synaptic structure and function can be impaired even by the smallest Aβ oligomers, called dimers (10). According to hydrogen/deuterium exchange experiments soluble oligomeric species exist in dynamic equilibrium with amyloid fibrils (11). These observations implicate a crucial role played by Aβ oligomers in amyloidogenesis.

Recognition of the importance of Aβ peptides in AD pathogenesis has led to a search of small molecular agents that can inhibit or delay Aβ aggregation. One of the potential antiaggregation agents is a nonsteroidal antiinflammatory drug naproxen (12) (Fig. 1 *a*). Long-term prophylactic use of naproxen may reduce the risk of AD (13–15). Reexamination of recent large-scale clinical trials revealed that when the patients with preexisting conditions are removed from consideration naproxen reduces the AD risk by 67% (12). However, it also appears that this drug offers no therapeutic effect in preexisting AD cases (16,17). In fact, according to mice models naproxen cannot reverse existing AD conditions in brain microglia (18). Several in vitro experimental studies have probed the interactions of naproxen with Aβ aggregates. In particular, experiments have implicated binding of naproxen to Aβ fibrils (19,20). Furthermore, naproxen has been shown to reduce the amount of Aβ fibrils upon its coincubation with the fresh Aβ monomers or to destabilize, but not to depolymerize, preformed Aβ fibrils (19,21). Experiments have also revealed that this nonsteroidal antiinflammatory drug interferes with Aβ fibril elongation and at a sufficiently large concentration completely inhibits fibril growth (21).

Although the antiaggregation effect of naproxen is documented, the underlying molecular mechanisms are unknown. In principle, molecular dynamics (MD) simulations can describe the interactions of Aβ species with the ligands at all-atom resolution (22). In recent years, MD was used to explore the mechanisms of fibril growth (23–26) and to investigate the conformational ensembles of amyloidogenic monomers (27,28) and oligomers (29–33). Recently, we have initiated a series of MD studies targeting the interactions between Aβ fibrils and naproxen ligands (34,35). We showed that naproxen binding to Aβ fibril is mainly governed by fibril surface geometry rather than by ligand-peptide interactions. In particular, the primary binding location of naproxen appears to be a hydrophobic groove located on the edge of growing Aβ fibril, which is also a preferred binding site for incoming Aβ peptides (26). Consequently, the antiaggregation effect of naproxen was explained by direct competition between the ligands and Aβ peptides for the same binding location on the fibril surface.

However, similar investigation of naproxen interactions with Aβ oligomers, which are the most cytotoxic species

Submitted December 22, 2010, and accepted for publication February 24, 2011.

*Correspondence: dklimov@gmu.edu

Editor: Ruth Nussinov.

0006-3495/11/04/2024/9 $2.00

doi: 10.1016/j.bpj.2011.02.044

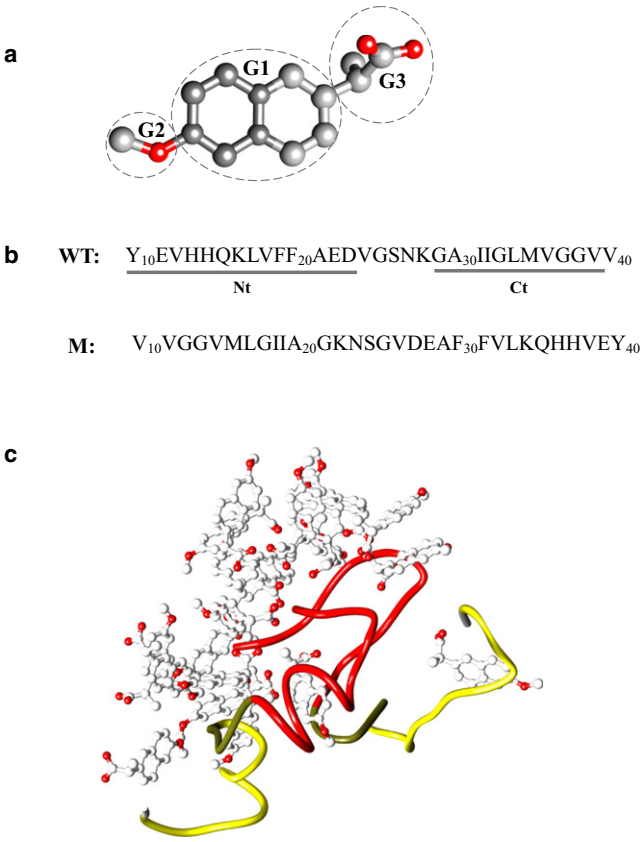

FIGURE 1 (*a*) Chemical structure of naproxen. Methoxy (G2) and carboxylate (G3) groups are linked to the central hydrophobic naphthalene ring (G1). Carbon and oxygen atoms are in gray and red (in online version). (*b*) The WT sequence of Aβ_{10-40} peptide and the allocation of the N- and C-terminals (Nt and Ct). In the mutant sequence the order of amino acids is reversed. (*c*) Typical structure of Aβ dimer coincubated with naproxen ligands at 360 K. Aβ Nt and Ct terminals are shown in red and yellow, respectively (in online version). Naproxen ligands bind with higher affinity to the N-terminal, which is also the primary dimer aggregation interface.

in AD, has not been performed. Therefore, it is not clear if naproxen destabilizes oligomers or even dissolves them. It is unknown if this ligand can selectively bind or recognize specific Aβ species, such as oligomers or fibrils. There is also no information on the location of naproxen binding sites in Aβ oligomers. From a more fundamental viewpoint, little is known about the physicochemical factors that control naproxen binding to Aβ oligomers, and if these factors are different from those governing binding to the fibril.

To answer these questions, we use exhaustive replica exchange MD (REMD) coupled with implicit solvent united atom model and study equilibrium interactions of Aβ dimers with naproxen ligands. We show that naproxen destabilizes Aβ dimer by penetrating into its core and interfering with interpeptide amino acid interactions. Based on the analysis of ligand binding energetics, we argue that the mechanism of naproxen binding to Aβ oligomer is different from that observed for the fibril. As a result, the affinity of naproxen binding to Aβ dimer is weaker compared to the fibril. We conclude with a discussion of naproxen antiaggregation efficiency with respect to different Aβ species.

METHODS

Simulation model

To simulate Aβ peptides coincubated with naproxen (Fig. 1), we used the CHARMM MD program (36) and united atom force field CHARMM19 coupled with the solvent accessible surface area (SASA) implicit solvent model (37). The force field description, its applicability, and testing can be found in our previous studies (31,34,38). In particular, we have shown that CHARMM19+SASA force field accurately reproduces the experimental distribution of chemical shifts for C_α and C_β atoms in Aβ monomers (31,39). Parameterization of naproxen (Fig. 1 *a*) in CHARMM19 force field was developed in the previous study (34). Additional arguments supporting the use of CHARMM19+SASA force field can be found in the Supporting Material.

In this work, we use the N-terminal truncated fragment of the full-length peptide, Aβ_{10-40} (Fig. 1 *b*) (40). The rationale for selecting Aβ_{10-40} as a model of the full-length Aβ_{1-40} is presented in the Supporting Material. The simulation system consists of two Aβ_{10-40} peptides interacting with 20 naproxen molecules (Fig. 1 *c*). Peptides and ligands are subject to spherical boundary condition with the radius $R_s = 90$ Å and the force constant $k_s = 10\ kcal\ /\ mol\ \text{Å}^2$. Consequently, the peptide and naproxen concentrations are $\approx$7 and 65 mM. The concentration ratio of naproxen to Aβ peptides, i.e., the ratio of the numbers of ligands and peptides is 10:1, which is within the range used experimentally (from 1 to 22) (21,41). Selection of Aβ dimer for our simulations is motivated by the experimental observation that the dimer is the smallest cytotoxic Aβ oligomer (10).

Replica exchange simulations

We used REMD to perform conformational sampling (42). The description of REMD implementation can be found in our previous studies (31,43). Briefly, 24 replicas were distributed linearly in the temperature range from 300 to 530 K with the increment of 10 K. The selected temperature range spans the spectrum of Aβ conformational states from aggregated to dissociate. Due to a small temperature increment the energy distributions from neighboring replicas share considerable overlap. The exchanges were attempted every 80 ps between all neighboring replicas with the average acceptance rate of 41%. In all, 13 REMD trajectories were produced resulting in the cumulative simulation time of 250 μs. The structures were saved with the interval of 40 ps, and between replica exchanges the system evolved using NVT underdamped Langevin dynamics with the damping coefficient $\gamma = 0.15\ \text{ps}^{-1}$ and the integration step of 2*fs*. Because initial parts of REMD trajectories are not equilibrated, the cumulative equilibrium simulation time is reduced to $\tau_{\text{sim}} \approx 227\ \mu$s. All REMD trajectories were started with random dissociated distributions of peptides and ligands in the sphere.

Computation of structural probes

Interactions formed by Aβ peptides and naproxen were probed as follows. A contact between amino acid side chains occurs, if the distance between their centers of mass is less than 6.5 Å. This cutoff approximately corresponds to the onset of hydration of side chains as their separation increases. If a contact involves two apolar amino acids, it is referred to as hydrophobic. A dimer is considered formed, if at least one side chain contact is established between the two peptides. Computations of contacts between naproxen and Aβ are described in the Supporting Material.

The backbone hydrogen bonds (HBs) between peptide NH and CO groups were assigned according to Kabsch and Sander (44). The same

definition was applied to detect HBs between naproxen and peptide backbone NH groups (34). Secondary structure in Aβ peptides was assigned using the distribution of (ϕ, ψ) backbone dihedral angles. Definitions of β-strand and helix states can be found in our earlier studies (31). The nonbonded energies of interactions between the ligands and between the ligands and Aβ were computed using CHARMM INTERACTION functionality. Definitions of radial distribution functions, $g_{pp}(r)$ and $g_{lp}(r)$, mapping minimum distances between amino acids and ligands, are given in the Supporting Material.

In our previous studies, assembly of Aβ dimer and Aβ fibril growth were studied in water at a temperature of 360 K, at which incoming Aβ peptide locks into fibril-like state during deposition onto the fibril (26,45). To facilitate the assessment of naproxen antiaggregation effect, we report the properties of Aβ dimers coincubated with naproxen at 360 K. However, we observed no qualitative differences in naproxen interactions with Aβ dimer, if the temperature is reduced to 330 K. To compute thermodynamic averages of structural quantities and free-energy landscapes the distributions of states produced by REMD were processed using the multiple histogram method (46). Throughout the article angular brackets <..> imply thermodynamic averages. Because dimer includes two indistinguishable peptides, quantities related to Aβ are averaged over two peptides. The convergence of REMD simulations and error analysis are presented in the Supporting Material.

Analysis of naproxen binding using AutoDock

To provide an independent test of naproxen binding mechanism, we used a software package AutoDock4.2 (47), which probed the interactions between Aβ peptide and naproxen. Details describing the application of AutoDock can be found in the Supporting Material.

RESULTS

Binding of naproxen and its impact on the stability of Aβ dimer were investigated using REMD simulations (Fig. 1 *c*). To assess changes in the structure of Aβ dimer and naproxen binding patterns, it is convenient to define the sequence regions in Aβ peptide. We distinguish the N-terminal (Nt, residues 10–23), which corresponds to the first β-strand in the Aβ fibril structure (48), and the C-terminal (Ct, residues 29–39), which corresponds to the second fibril β-strand (Fig. 1 *b*).

Naproxen destabilizes Aβ dimer

To examine the assembly of Aβ dimer coincubated with naproxen, we computed the number of interpeptide contacts $\langle C(T)\rangle$ and interpeptide hydrophobic contacts $\langle C_h(T)\rangle$ as a function of temperature T and compared them with the same quantities $\langle C(T;w)\rangle$ and $\langle C_h(T;w)\rangle$ obtained in water (45). Fig. 2 shows that $\langle C(T)\rangle$ and $\langle C(T;w)\rangle$ increase with the decrease in T and are similar up to $T \gtrsim 400$ K. At lower temperatures the number of interpeptide contacts in water $\langle C(T;w)\rangle$ continues its monotonic increase, whereas $\langle C(T)\rangle$ declines. Similar behavior is seen in the temperature dependence of interpeptide hydrophobic contacts $\langle C_h(T)\rangle$. At 360 K the number of interpeptide side chain contacts in Aβ dimer coincubated in naproxen and in water are $\langle C\rangle \approx 19.8$ and $\langle C(w)\rangle \approx 30.0$, respectively. Similarly, the

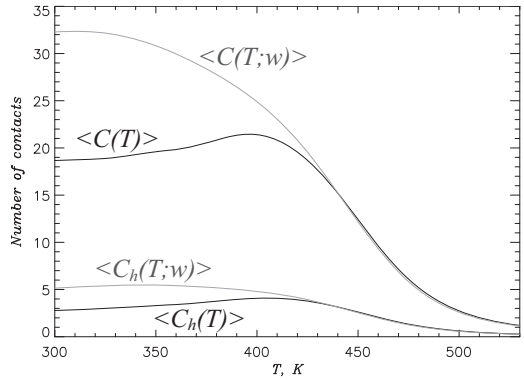

FIGURE 2 Formation of Aβ_{10-40} dimer is probed using the temperature dependencies of the numbers of interpeptide side chain contacts $\langle C(T)\rangle$ and interpeptide hydrophobic contacts $\langle C_h(T)\rangle$. Data in black and gray correspond to naproxen solution and ligand-free water, respectively. The plot demonstrates that naproxen interference weakens interpeptide interactions.

number of interpeptide hydrophobic contacts is reduced from 5.4 in water to 3.4 in naproxen. This implies that naproxen eliminates approximately one-third of interpeptide interactions. The antiaggregation effect of naproxen appears to increase with the decrease in temperature.

The impact of naproxen is further probed by computing the free energy of Aβ dimer, $F(C)$, as a function of the number of interpeptide contacts C. Similar to the free energy profiles we computed for the ligand-free (water) environment (45), $F(C)$ features a single minimum attributed to dimer state. The free energy of dimer formation is defined as $\Delta F_{A-D} = F_A - F_D$, where F_A and $F_D = 0$ are the free energies of associated (A) and dissociated (D, $C = 0$) states. To compute F_A we integrated the states with $F(C) \leq F_{\min} + 1.0\,RT$, where $F_{\min}$ is the minimum in $F(C)$. When Aβ peptides are coincubated with naproxen at 360 K, $\Delta F_{A-D}(npxn)$ is $\approx -6.1\,RT$ compared to $\Delta F_{A-D}(w) \approx -7.5\,RT$ in water (45). Therefore, naproxen interactions reduce the free energy of dimer formation by $\Delta\Delta F_{A-D} = \Delta F_{A-D}(npxn) - \Delta F_{A-D}(w) \approx 1.4\,RT$. Consistent with the growing gap between $\langle C(T)\rangle$ and $\langle C(T;w)\rangle$ in Fig. 2, at 330 K, $\Delta\Delta F_{A-D}$ increases to $5.4\,RT$.

Structural changes in Aβ oligomer induced by naproxen can be revealed by computing the radial number density $G(r)$ of Aβ atoms as a function of the distance to the oligomer center of mass r. Fig. 3 *a* shows that $G(r)$ remains relatively constant at $r \lesssim 10$ A and then sharply declines. Consequently, we define the dimer core, in which the atomic density is approximately constant, using the condition $G(r_c) = 0.7\,G(0)$, where r_c is the core radius. We found that at 360 K $r_c = 12$ A. To study the changes in the dimer size, the inset to Fig. 3 *a* displays the temperature dependences of the core volumes computed for naproxen solution and water (49), $V_c(T)$ and $V_c(T;w)$, respectively. At $T \lesssim 400$ K, the Aβ dimer coincubated with naproxen expands compared to the ligand-free environment. For instance, V_c exceeds $V_c(w)$ by ~30% at 360 K. The reason

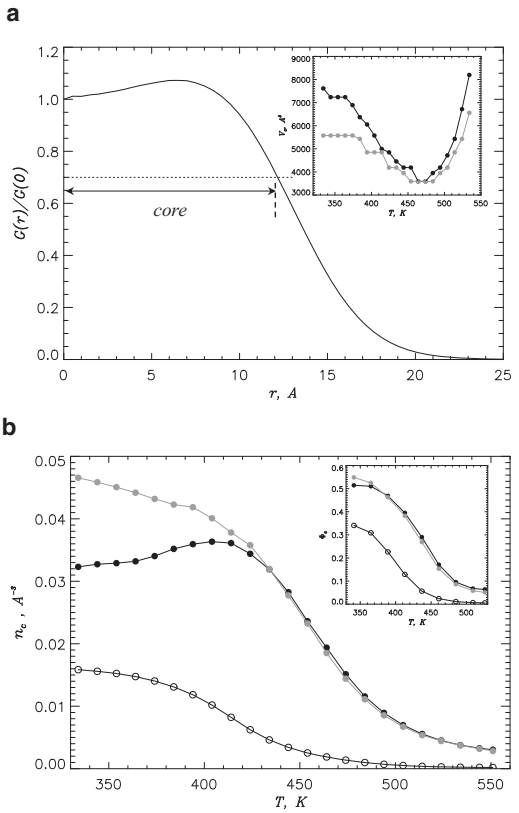

FIGURE 3 (*a*) Normalized radial number density $G(r)$ of Aβ atoms as a function of the distance to the dimer center of mass r at 360 K. Dotted line marks the level of $0.7G(0)$ used to define the dimer core. Inset shows the temperature dependence of the core volume: $V_c(T)$(in *black*) for naproxen solution, $V_c(T;w)$(in *gray*) for water. (*b*) Peptide atom number density in the core as a function of temperature: $n_c(T)$(*black solid circles*) for naproxen solution, $n_c(T;w)$(*gray circles*) for water. Ligand atom number density $n_c(T;npxn)$ in the core is shown by open circles. Inset displays the fraction of peptide atoms in the dimer core $\Phi_c(T)$ versus temperature: naproxen solution (*solid black circles*), water (*gray circles*). The fraction of ligand atoms in the core $\Phi_c(T;npxn)$ is shown by open circles. The figure indicates that the dimer expansion is accompanied by the drop of peptide atom density and penetration of ligands into its core.

for dimer swelling can be gleaned from Fig. 3 *b*. The inset shows the fractions of Aβ atoms $\Phi_c(T)$ in the dimer core as a function of temperature in naproxen solution and water. This plot suggests that $\Phi_c(T)$ is not affected by naproxen. However, if one considers the average peptide atom number density in the core computed for naproxen solution and water, $n_c(T)$ and $n_c(T;w)$, it then becomes clear that $n_c(T)$ is reduced ~25% compared to water at 360 K (Fig. 3 *b*). We observe from Fig. 3 *b* that the decrease in peptide atom density is accompanied by the increase in the ligand atom density in the core $n_c(T;npxn)$, i.e., by the influx of ligands into the dimer volume. Specifically, the inset to Fig. 3 *b* demonstrates that 32% of naproxen molecules ($\Phi_c(npxn) = 0.32$) are localized in the dimer core at 360 K. Therefore, expansion of the dimer is caused by penetration of ligands into its core.

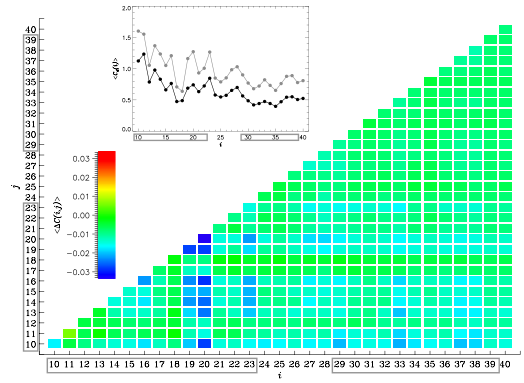

FIGURE 4 Difference contact map $\langle\Delta C(i,j)\rangle$ shows changes in the probabilities of interpeptide contacts between residues i and j in Aβ dimer at 360 K. Values of $\langle\Delta C(i,j)\rangle$ are color coded according to the scale. The inset displays the numbers of interpeptide contacts formed by residues i in Aβ dimer: $\langle C_d(i)\rangle$(in *black*) for naproxen solution, $\langle C_d(i;w)\rangle$(in *gray*) for water. The Nt and Ct terminals are boxed. These plots reveal that naproxen weakens interpeptide interactions, but does not shift the dimer aggregation interface, which is still centered in the Nt.

To investigate the impact of naproxen on the dimer aggregation interface, we analyzed the difference contact map $\langle\Delta C(i,j)\rangle$, which shows the changes in the probabilities of interpeptide contacts formed by residues i and j in naproxen solution relative to water. Fig. 4 shows that naproxen either reduces the probability of interpeptide contacts or leaves them intact. The inset to Fig. 4 compares the number of interpeptide contacts, $\langle C_d(i)\rangle$ and $\langle C_d(i;w)\rangle$, formed by residues i in Aβ dimer in naproxen solution and water, respectively. The naproxen weakens interpeptide interactions in both the Nt and Ct terminals. For example, the total numbers of interpeptide contacts in the Nt and Ct are reduced by 5.1 (a 32% decrease with respect to water value) and 3.3 (a 38% decrease), respectively. The largest decreases in contact numbers are observed for Phe20, Phe19, and Tyr10. However, naproxen interference does not change the location of Aβ aggregation interface. Specifically, $<C_d(Nt)> = 11.0$ and $<C_d(Ct)> = 5.3$ interpeptide contacts in naproxen solution are formed by Aβ Nt and Ct terminals. For comparison, in water the corresponding numbers are 16.1 and 8.6. Therefore, in both environments $\langle C_d(Nt)\rangle/\langle C_d(Ct)\rangle \approx 2$ indicating that about two-thirds of interpeptide interactions are localized in the Nt terminal, i.e., this sequence region is the primary aggregation interface in water and in naproxen solution. Furthermore, this point can be illustrated if one considers the probability $P_c(i)$ for amino acid i to occur in the dimer core of the radius r_c. Fig. S3 shows that $P_c(i)$ and $P_c(i;w)$ computed for naproxen solution and water (49) are remarkably similar. For example, in naproxen solution at 360 K the average P_c for the residues in the Nt and Ct are 0.57 and 0.35. The same quantities computed for water are 0.57 and 0.40 (49). Hence, in both environments the Nt terminal is typically buried in the dimer core, whereas the Ct is exposed.

The changes in secondary structure induced by naproxen are assessed by computing the fractions of β-strand and helix residues, $\langle S \rangle$ and $\langle H \rangle$, at 360 K. In naproxen solution, $\langle S \rangle$ and $\langle H \rangle$ are 0.40 and 0.18 compared to 0.37 and 0.21 in water (45). The largest change in secondary structure is observed in the Nt, where the strand content $\langle S(Nt) \rangle$ increases from 0.36 in water to 0.44 in naproxen solution. Simultaneously, $\langle H(Nt) \rangle$ is decreased from 0.32 to 0.25. However, on average naproxen induces conformational change in only two residues in Aβ peptide within the dimer, so its secondary structure remains largely unchanged.

Naproxen binding to Aβ dimer affects interpeptide interactions

Destabilization of Aβ dimer by naproxen suggests binding of this ligand to Aβ. To examine naproxen-Aβ interactions, we plot the probability of naproxen molecule binding to Aβ dimer, P_b (Fig. 5 *a*). Defining the binding temperature T_b from the condition $P_b(T_b) = 0.5$, we find $T_b = 380$ K; because at 360 K $P_b \approx 0.71$, the average number of bound ligands is $\langle L \rangle \approx 14.2$ (out of the total of 20). It is important that ~45% of the bound ligands ($\langle L_i \rangle \approx 6.3$) interfere with the interpeptide interactions as they bind simultaneously to both peptides in the dimer (inset to Fig. 5 *a*). Given that the total number of contacts between naproxen and Aβ dimer is $\langle C_l \rangle \approx 58.8$, each bound naproxen ligand interacts with roughly four amino acids. Interestingly, the contribution of ligand-Aβ HBs to binding is small. For example, the total number of HBs between the ligands and Aβ dimer backbone at 360 K is only $\langle N_{lhb} \rangle \approx 3.5$, i.e., it is 16 times smaller than $\langle C_l \rangle$.

As a quantitative measure of naproxen binding affinity we use the binding free energy ΔF_b, which is the difference between the free energies of the bound and unbound states. This can be obtained from the free energy $F(r_b)$ of a ligand as a function of the distance between ligand and Aβ dimer, r_b (Fig. 5 *b*). The profile of $F(r_b)$ displays a single minimum at $r_b \approx 5$ Å attributed to the bound state, from which ΔF_b is found to be $-6.8\,RT$.

Our simulations indicate that naproxen molecules penetrate the volume of Aβ dimer and almost half impact the dimer aggregation interface. Further illustration of the competition between interpeptide amino acid interactions and ligands-peptide contacts comes from the analysis of amino acid and ligand radial distribution functions, $g_{pp}(r)$ and $g_{lp}(r)$ (the inset to Fig. 5 *b*). It follows from $g_{pp}(r)$ that a contact distance between amino acids from different peptides in water peaks at $r \approx 5$ A. When coincubated with naproxen, the amplitude of the $g_{pp}(r)$ peak is reduced and its tail extends to a larger r. Of importance, the function $g_{lp}(r)$, which measures the distribution of contact distances r between naproxen ligands and amino acids, reveals that a typical r coincides with that observed for amino acid interpeptide contacts. The comparison of these functions suggests that 1) a direct competition between interpeptide amino acid and ligands-peptide interactions takes place and 2) interpeptide amino acid contacts are suppressed and the separation between amino acids grows (from 7.8 in water to 9.1 A in naproxen solution).

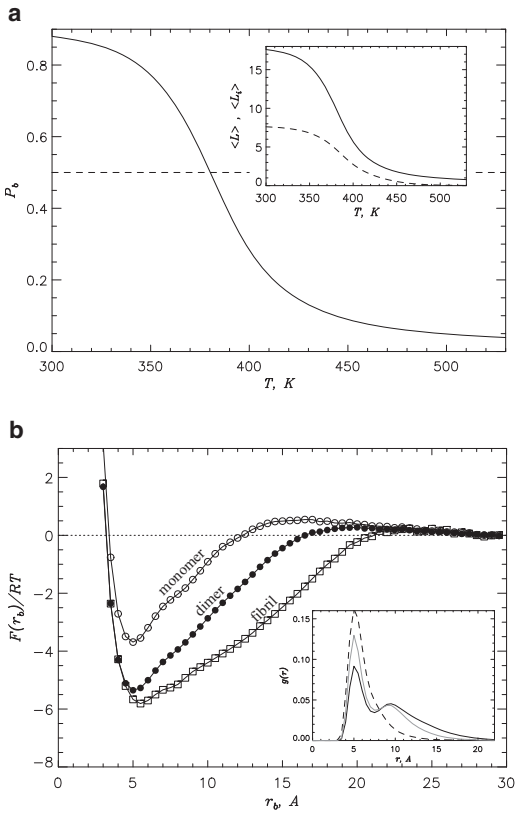

FIGURE 5 (*a*) Probability of naproxen molecule binding to Aβ dimer, $P_b(T)$, as a function of temperature. Binding temperature T_b is associated with the midpoint of $P_b(T)$. Inset shows the number of naproxen ligands bound to Aβ dimer $\langle L \rangle$ (*continuous line*) and the number of ligands bound to Aβ aggregation interface $\langle L_i \rangle$ (*dashed line*) versus temperature. (*b*) Free energy $F(r_b)$ of naproxen as a function of the distance between ligand and Aβ dimer, r_b (*solid circles*). The free energy of binding ΔF_b is computed by integrating over the ligand bound states with $F(r_b) \leq F_{\min} + 1.0\,RT$, where $F_{\min}$ is the minimum in $F(r_b)$. The values of F at r_b>29 Å are set to zero and correspond to unbound state. Free energies $F(r_b)$ describing naproxen binding to Aβ monomer and fibril computed earlier (35) are given by open circles and squares, respectively. Inset: Radial distribution functions, $g_{pp}(r)$ and $g_{lp}(r)$, map minimum distances between amino acids from different peptides and between ligands and amino acids, respectively. The functions $g_{pp}(r)$ obtained in water and naproxen solution are shown by continuous gray and black lines; the function $g_{lp}(r)$ is represented by a dashed line. All plots in (*b*) are obtained at 360 K. The figure implies that naproxen binds to Aβ dimer and interferes with interpeptide interactions.

Naproxen binding to Aβ dimer is governed by Aβ sequence

It is important to establish the factors that control naproxen binding to Aβ dimer. To this end, we use a combination of implicit solvent REMD and AutoDock simulations (see Methods). Because the latter were performed at 330 K, we report corresponding REMD data at the lower temperature

of 330 K, which is closer to physiological regime. (As emphasized above, naproxen binding propensities at 330 and 360 K are qualitatively similar.) We first analyze the binding affinities of residues in Aβ sequence. Fig. 6 *a* presents the number of contacts $\langle C_l(i)\rangle$ formed by amino acid i with the ligands. Despite noticeable fluctuations in $\langle C_l(i)\rangle$, with i it is clear that the N-terminal forms contacts with naproxen more frequently than the C-terminal. Specifically, the Nt and Ct regions form 19.9 and 8.6 contacts, respectively, or 1.4 and 0.8 contacts per residue. To check if ligand binding is driven by the interactions with side chains, we plot in Fig. 6 *a* the energies of interactions between amino acid i and ligands $\langle E_b(i)\rangle$. This figure reveals a strong correlation between $\langle C_l(i)\rangle$ and $\langle E_b(i)\rangle$ (the correlation factor is 0.94). Consistent with the distribution of ligand-residue contacts $\langle C_l(i)\rangle$ the N-terminal forms significantly stronger interactions with naproxen than the Ct. For example, the average ligands-residue energy for amino acid in the Nt is $\langle E_b(Nt)\rangle \approx -4.1\ kcal/mol$, whereas the ligands-residue interactions in the Ct are three times weaker ($\langle E_b(Ct)\rangle \approx -1.3\ kcal/mol$). To check if the naproxen binding is affected by the local secondary structure, we compared the fractions of strand and helix structure for individual residues, $\langle S(i)\rangle$ and $\langle H(i)\rangle$, with $\langle C_l(i)\rangle$. The absolute values of correlation coefficients computed for $(\langle S(i)\rangle, \langle C_l(i)\rangle)$ and $(\langle H(i)\rangle, \langle C_l(i)\rangle)$ pairs are less than 0.1, suggesting that Aβ secondary structure has no impact on naproxen binding.

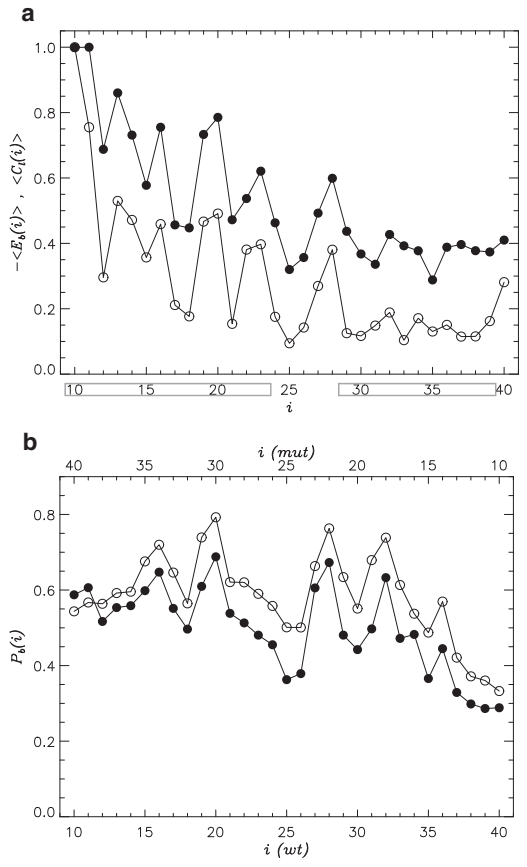

FIGURE 6 (*a*) Number of contacts $\langle C_l(i)\rangle$ formed by amino acid i in Aβ dimer with naproxen ligands (*solid circles*). Energy of interactions between amino acid i and ligands $\langle E_b(i)\rangle$ are represented by open circles. Both quantities are computed using REMD at 330 K and normalized. The Nt and Ct terminals are boxed. (*b*) Probability $P_b(i)$ of naproxen binding to amino acid i in Aβ monomer computed using AutoDock: WT Aβ (*solid circles*), reversed Aβ mutant (*open circles*, Fig. 1 *b*). Amino acid numbers for the mutant sequence are shown on top in a backward direction (from 40 to 10). Both panels implicate ligand-amino acid interactions as a main factor controlling the location of ligand binding sites along Aβ sequence.

Our previous studies of naproxen binding to Aβ fibrils have determined that interligand interactions make a large contribution to binding energetics (34). To probe the interactions between naproxen molecules we examined the formation of ligand clusters bound to Aβ dimer. A bound cluster of the size S_c is defined as a group of S_c interacting ligands, among which at least one is bound to Aβ. The distribution of the number of ligands $\langle L(S_c)\rangle$ with respect to the cluster size S_c is bimodal at 330 K (see Fig. S4). About 92% of ligands are involved in large clusters (S_c>6) that implicates strong interligand interactions. Indeed, for a bound naproxen the average energy of ligand-ligand interactions is $\langle E_{ll}\rangle \approx -14.7\ kcal/mol$, whereas the energy of ligand-Aβ interactions is smaller ($\langle E_{lp}\rangle \approx -8.0\ kcal/mol$). To establish the roles of these interactions in binding to Aβ, we computed $\langle E_{ll}\rangle$ and $\langle E_{lp}\rangle$ separately for the naproxen molecules bound to the Nt and Ct regions. The average ligand-ligand energies $\langle E_{ll}\rangle$ for naproxen molecules bound to the Nt and Ct are similar ($<\Delta E_{ll}> = <E_{ll}(Nt)> - E_{ll}(Ct)> \approx -1.0\ kcal/mol$). In contrast, the corresponding difference in the ligand-Aβ energy $\langle \Delta E_{lp}\rangle$ is three-fold larger ($-3.3\ kcal/mol$) consistent with the computations of ligands-residue interactions in Fig. 6 *a*.

Our results suggest that the interactions between naproxen ligands and Aβ side chains determine the distribution of naproxen along the Aβ sequence. To provide an additional test for this conclusion, we use the AutoDock simulations and consider the probability $P_b(i)$ of naproxen binding to amino acid i in Aβ monomer (see Methods). These computations were performed for the wild-type (WT) Aβ sequence and the mutant, in which the order of amino acids is reversed (Fig. 1 *b*). Reversed sequence is "fitted" into the monomer structures (see Supporting Material). If binding of naproxen to Aβ is driven by the interactions with amino acids, then the mutant profile $P_b^M(i)$ should also be reversed as a function of i when compared to the WT $P_b(i)$. To check this assumption, Fig. 6 *b* superimposes the WT and mutant probability distributions $P_b(i)$ and $P_b^M(i)$. It is clear that both profiles are remarkably similar when the WT sequence is compared with the backward counted mutant one (the corresponding correlation coefficient is 0.91). These computations together with the data presented above implicate the interactions between ligands and amino acids as the main factor controlling the distribution of naproxen binding sites in Aβ dimer.

DISCUSSION

Mechanism of naproxen antiaggregation effect

In this article, we have analyzed binding of naproxen to Aβ dimer, the smallest Aβ oligomer. Our REMD simulations indicate that naproxen binds to Aβ dimer at temperatures below $T_b = 380$ K. Naproxen binding destabilizes, but does not depolymerize Aβ dimer. At 360 K naproxen interference eliminates about one-third of the interpeptide interactions in the dimer and reduces the free energy gain of dimer formation ΔF_{A-D} by $\Delta\Delta F_{A-D} = 1.4\,RT$, from -7.5 to $-6.1\,RT$. We further showed that about a third of all naproxen ligands penetrate the core of Aβ dimer, causing a 30% swelling of its volume. Of importance, these structural changes result in ~25% drop of the peptide atom number density in the core. Our simulations also suggest that close to half of the bound ligands (45%) occur at the Aβ dimer interface resulting in a direct competition between ligand-amino acid and amino acid-amino acid interactions (Fig. 5 *b*). Consequently, interpeptide side chain contacts are compromised. Direct interference of ligands with interpeptide interactions has been also observed for tricyclic planar ligands (50). MD simulations have shown that 9,10-anthraquinone binding to Aβ_{14-20} peptide destabilizes the formation of interstrand HBs and reduces the accumulation of ordered aggregates.

Comparison of the free energies of ligand binding and dimer formation can explain why naproxen only destabilizes Aβ dimer. According to our previous simulations (34) the free energy of naproxen binding to Aβ monomer $\Delta F_b(m)$ is $-5.1\,RT$ (Fig. 5 *b*). This value should be compared with the free energy of dimer formation in water, which is $\Delta F_{A-D}(w) = -7.5\,RT$ (45). Therefore, the affinity of Aβ peptide with respect to binding naproxen is weaker than for binding another Aβ chain.

An interesting question pertains to the comparison of antiaggregation propensity of naproxen against Aβ dimers and fibrils. Recently, we have studied the growth of Aβ amyloid fibril in naproxen solution and compared it with the ligand-free environment (35). It has been shown that naproxen reduces the free energy of Aβ binding to the fibril ΔF_{B-U} by $\Delta\Delta F_{B-U} = 5.2\,RT$, from -9.9 in water to $-4.7\,RT$ in naproxen solution. In contrast, at the same conditions and for the same ligand:peptide ratio naproxen reduces the dimer aggregation free energy to $\Delta F_{A-D} = -6.1\,RT$ (i.e., only by $1.4\,RT$ as shown above). Therefore, in naproxen solution Aβ dimer has lower free energy than Aβ peptide bound to amyloid fibril. It is also worth noting two other observations. First, the free energy of naproxen binding to Aβ monomer $\Delta F_b(m) = -5.1\,RT$ is higher than that of ligand binding to Aβ fibril ($\Delta F_b(f) = -7.6\,RT$, Fig. 5 *b*) (34). Second, due to naproxen the number of peptide-fibril side chain contacts is reduced by 14.9 (35), whereas the number of interpeptide contacts in the dimer is reduced by 10.2. These findings imply that naproxen works as a better antiaggregation agent against Aβ fibrils than against oligomers. It is also expected that, although the decrease in naproxen concentration will weaken its antiaggregation propensity, the relative antiaggregation efficiency against Aβ fibrils and oligomers will not change.

Our REMD simulations suggest that naproxen does not change aggregation interface of Aβ dimer. This inference is based on two results. First, as in water (45) the aggregation interface primarily involves the Aβ Nt terminal, which forms about two-thirds of the interpeptide interactions (Fig. 4). Second, the spatial distributions of amino acids in the dimer volume $P_c(i)$ reveal the same propensities for the Nt and Ct terminals to occur in the dimer core in both environments (Fig. S3) (49). As a rule the core is formed by the Nt, whereas the Ct is mainly found on the dimer surface. Furthermore, our analysis indicates that naproxen binding does not change the distribution of Aβ dimer conformational clusters compared to water environment (45). This observation is likely the result of the lack of correlation between the Aβ secondary structure and naproxen binding.

Finally, it is interesting to comment on the secondary structure changes induced by naproxen in different Aβ species. Naproxen appears to make minor changes in β-strand and helix contents in the dimer (<15%, see Results) and in Aβ peptides bound to the fibril (<6%) (35). In contrast, naproxen induces a shift in the monomer conformational ensemble, increasing the β content by 50% and decreasing the helix population by a third (35). Thus, naproxen binding has a noticeable impact on the Aβ monomer conformations, but small on aggregated species.

Naproxen binds to Aβ dimers and fibrils via different mechanisms

Are the mechanisms of naproxen binding to Aβ dimers and fibril different? Our previous studies of naproxen interactions with Aβ fibrils (34) and the current work allow us to examine this question. Aβ fibril features concave (CV) and convex (CX) edges, which have different binding affinities for naproxen. The number of ligands bound to the CV edge, which has a groove, is more than twice larger than the number of ligands attracted to the CX with a protruding surface. Of importance, the energies of ligand-fibril interactions are similar for the CX and CV edges. In contrast, the energy of ligand-ligand interactions for the CV is 5.5 $kcal\,/\,mol$ lower compared to the CX edge. As a result binding to the CV edge is energetically preferred. We showed previously that the enhancement of interligand interactions on the CV edge is the result of the confinement effect of the groove, which induces the formation of large clusters of bound ligands (34,51). At 360 K ~90% of bound naproxen molecules participate in the formation of large clusters (S_c>6). This previous energetics analysis together with the computational study of thioflavin-T binding (52) showed that the location of ligand binding sites on amyloid

fibril is mainly determined by its surface geometry, rather than by sequence.

Study of naproxen binding to Aβ dimer also reveals strong intermolecular interactions formed between bound naproxen ligands. For example, the energy of ligand-ligand interactions $\langle E_{ll} \rangle$ is approximately two times lower than the ligand-Aβ interaction energy $\langle E_{lp} \rangle$. Furthermore, on an average 92% of ligands form large clusters bound to Aβ dimer. These aspects of naproxen binding to Aβ dimer are similar to the fibril binding. The difference is the interactions between the ligands and amino acids in Aβ dimer appear to control the location of binding sites. There are three lines of evidence to this conclusion. First, the change in the energy of interligand interactions $\langle E_{ll} \rangle$ along the Aβ sequence is three times smaller than the corresponding variation in the energy of ligand-residue interactions $\langle E_{lp} \rangle$. Second, Fig. 6 *a* strongly suggests that the distribution of ligand binding sites along the Aβ sequence is determined by the energies of interactions between ligands and amino acids. Third, the distributions of bound ligands along the WT and reversed Aβ sequences are in close agreement when the reversed sequence is considered in the backward direction (Fig. 6 *b*). These observations imply that the binding sites follow the sequence of amino acids. On the basis of our analysis, we argue that the preferential binding location of naproxen in Aβ dimer is the N-terminal, which is also the primary aggregation interface. This circumstance contributes to the antiaggregation propensity of naproxen.

Because Aβ dimer has fluid structure, the formation of stable grooves is unlikely. Therefore, even though naproxen forms attractive interligand interactions upon binding to Aβ dimer, these interactions cannot determine the location of binding sites as it occurs for Aβ fibril. The arguments presented above suggest that the mechanisms of naproxen binding to Aβ oligomers and fibrils are different.

Comparison with experiments

It is important to compare our in silico findings with available experimental data. We are not aware of the experiments that have specifically investigated the impact of naproxen on Aβ oligomers. However, studies of other ligands may provide important insights into naproxen antiaggregation potential. For example, the effect of curcumin, a ligand with two phenyl rings, on Aβ aggregation has been studied (53). It has been demonstrated that curcumin completely blocks Aβ oligomer formation at the ligand to the Aβ stoichiometric ratio of 3:1. It was also reported that curcumin reduces but does not prevent fibril formation. Furthermore, according to the experiments curcumin inhibits Aβ cytotoxicity at the stoichiometric ratio of 10:1. Based on the comparison of the concentrations of curcumin and naproxen, which achieve the same inhibition of Aβ aggregation, the latter was found to be a four times less potent antiaggregation agent than curcumin.

It seems likely that the reason for relative inefficiency of naproxen compared to curcumin is its weaker antiaggregation propensity against Aβ oligomers compared to that against Aβ fibrils. Recent experiments indicate that such a mode of antiaggregation is not optimal for blocking Aβ cytotoxicity. For example, Hecht and co-workers have found that the ligands, which provide the strongest inhibition of cytotoxicity, are those that accelerate fibril formation (54). Compared to naproxen these compounds are likely to reduce more efficiently the concentration of Aβ oligomers, which are the primary cytotoxic Aβ species as shown in recent mutagenesis studies with murine models (9). In contrast, according to our data naproxen destabilizes less cytotoxic Aβ fibrils to a greater extent than the most cytotoxic Aβ oligomers. This antiaggregation effect may even be counterproductive as it may raise the concentration of oligomeric species. Therefore, according to our study the limitations of naproxen as an antiaggregation agent are that 1) it targets Aβ fibrils rather than oligomers and 2) it destabilizes but does not dissociate Aβ aggregates. These circumstances might be the reasons for naproxen moderate efficiency as prophylactic therapeutic agent in AD, and its failure to reverse preexisting AD conditions (12,15).

SUPPORTING MATERIAL

Additional details, arguments, rationale, computations, definitions, four figures, and references are available at http://www.biophysj.org/biophysj/supplemental/S0006-3495(11)00295-5.

We thank Takako Takeda for help with the analysis of binding energetics.

This work was supported by the National Institute on Aging (National Institutes of Health) (grant R01 AG028191). The content is solely the responsibility of the authors and does not necessarily represent the official views of the National Institute on Aging or the National Institutes of Health.

REFERENCES

1. Selkoe, D. J. 2003. Folding proteins in fatal ways. *Nature.* 426:900–904.
2. Dobson, C. M. 2003. Protein folding and misfolding. *Nature.* 426:884–890.
3. Hardy, J., and D. J. Selkoe. 2002. The amyloid hypothesis of Alzheimer's disease: progress and problems on the road to therapeutics. *Science.* 297:353–356.
4. Kirkitadze, M. D., G. Bitan, and D. B. Teplow. 2002. Paradigm shifts in Alzheimer's disease and other neurodegenerative disorders: the emerging role of oligomeric assemblies. *J. Neurosci. Res.* 69:567–577.
5. Murphy, R. M. 2002. Peptide aggregation in neurodegenerative disease. *Annu. Rev. Biomed. Eng.* 4:155–174.
6. Hardy, J. A., and G. A. Higgins. 1992. Alzheimer's disease: the amyloid cascade hypothesis. *Science.* 256:184–185.
7. Kayed, R., E. Head, …, C. G. Glabe. 2003. Common structure of soluble amyloid oligomers implies common mechanism of pathogenesis. *Science.* 300:486–489.
8. Haass, C., and D. J. Selkoe. 2007. Soluble protein oligomers in neurodegeneration: lessons from the Alzheimer's amyloid β-peptide. *Nat. Rev. Mol. Cell Biol.* 8:101–112.
9. Gandy, S., A. J. Simon, …, M. E. Ehrlich. 2010. Days to criterion as an indicator of toxicity associated with human Alzheimer amyloid-beta oligomers. *Ann. Neurol.* 68:220–230.

10. Shankar, G. M., S. Li, …, D. J. Selkoe. 2008. Amyloid-β protein dimers isolated directly from Alzheimer's brains impair synaptic plasticity and memory. *Nat. Med.* 14:837–842.
11. Carulla, N., G. L. Caddy, …, C. M. Dobson. 2005. Molecular recycling within amyloid fibrils. *Nature.* 436:554–558.
12. Cole, G. M., and S. A. Frautschy. 2010. Mechanisms of action of non-steroidal anti-inflammatory drugs for the prevention of Alzheimer's disease. *CNS Neurol. Disord. Drug Targets.* 9:140–148.
13. Vlad, S. C., D. R. Miller, …, D. T. Felson. 2008. Protective effects of NSAIDs on the development of Alzheimer disease. *Neurology.* 70:1672–1677.
14. Imbimbo, B. P. 2009. An update on the efficacy of non-steroidal anti-inflammatory drugs in Alzheimer's disease. *Expert Opin. Investig. Drugs.* 18:1147–1168.
15. Imbimbo, B. P., V. Solfrizzi, and F. Panza. 2010. Are NSAIDs useful to treat Alzheimer's disease or mild cognitive impairment? *Front. Aging Neurosci.* 2:1–14.
16. Imbimbo, B. P. 2004. The potential role of non-steroidal anti-inflammatory drugs in treating Alzheimer's disease. *Expert Opin. Investig. Drugs.* 13:1469–1481.
17. Gasparini, L., E. Ongini, and G. Wenk. 2004. Non-steroidal anti-inflammatory drugs (NSAIDs) in Alzheimer's disease: old and new mechanisms of action. *J. Neurochem.* 91:521–536.
18. Varvel, N. H., K. Bhaskar, …, K. Herrup. 2009. NSAIDs prevent, but do not reverse, neuronal cell cycle reentry in a mouse model of Alzheimer disease. *J. Clin. Invest.* 119:3692–3702.
19. Agdeppa, E. D., V. Kepe, …, J. R. Barrio. 2003. In vitro detection of (s)-naproxen and ibuprofen binding to plaques in the Alzheimer's brain using the positron emission tomography molecular imaging probe 2-(1-{6-[(2-[18F]fluoroethyl)(methyl)amino]-2-naphthyl}ethylidene) malononitrile. *Neuroscience.* 117:723–730.
20. LeVine, 3rd, H. 2005. Multiple ligand binding sites on Aβ(1-40) fibrils. *Amyloid.* 12:5–14.
21. Hirohata, M., K. Ono, …, M. Yamada. 2005. Non-steroidal anti-inflammatory drugs have anti-amyloidogenic effects for Alzheimer's β-amyloid fibrils in vitro. *Neuropharmacology.* 49:1088–1099.
22. Ma, B., and R. Nussinov. 2006. Simulations as analytical tools to understand protein aggregation and predict amyloid conformation. *Curr. Opin. Chem. Biol.* 10:445–452.
23. Cecchini, M., F. Rao, …, A. Caflisch. 2004. Replica exchange molecular dynamics simulations of amyloid peptide aggregation. *J. Chem. Phys.* 121:10748–10756.
24. Nguyen, P. H., M. S. Li, …, D. Thirumalai. 2007. Monomer adds to preformed structured oligomers of Abeta-peptides by a two-stage dock-lock mechanism. *Proc. Natl. Acad. Sci. USA.* 104:111–116.
25. Krone, M. G., L. Hua, …, J. E. Shea. 2008. Role of water in mediating the assembly of Alzheimer amyloid-beta Abeta16-22 protofilaments. *J. Am. Chem. Soc.* 130:11066–11072. 10.1021/ja8017303.
26. Takeda, T., and D. K. Klimov. 2009. Replica exchange simulations of the thermodynamics of Abeta fibril growth. *Biophys. J.* 96:442–452.
27. Sgourakis, N. G., Y. Yan, …, A. E. Garcia. 2007. The Alzheimer's peptides Abeta40 and 42 adopt distinct conformations in water: a combined MD / NMR study. *J. Mol. Biol.* 368:1448–1457.
28. Yang, M., and D. B. Teplow. 2008. Amyloid β-protein monomer folding: free-energy surfaces reveal alloform-specific differences. *J. Mol. Biol.* 384:450–464.
29. Lu, Y., P. Derreumaux, …, G. Wei. 2009. Thermodynamics and dynamics of amyloid peptide oligomerization are sequence dependent. *Proteins.* 75:954–963.
30. Bellesia, G., and J.-E. Shea. 2009. What determines the structure and stability of KFFE monomers, dimers, and protofibrils? *Biophys. J.* 96: 875–886.
31. Takeda, T., and D. K. Klimov. 2009. Interpeptide interactions induce helix to strand structural transition in Abeta peptides. *Proteins.* 77:1–13.
32. Anand, P., F. S. Nandel, and U. H. E. Hansmann. 2008. The Alzheimer β-amyloid (Abeta(1-39)) dimer in an implicit solvent. *J. Chem. Phys.* 129:195102.
33. Urbanc, B., M. Betnel, …, D. B. Teplow. 2010. Elucidation of amyloid β-protein oligomerization mechanisms: discrete molecular dynamics study. *J. Am. Chem. Soc.* 132:4266–4280.
34. Takeda, T., W. E. Chang, …, D. K. Klimov. 2010. Binding of non-steroidal anti-inflammatory drugs to Abeta fibril. *Proteins.* 78:2859–2860.
35. Takeda, T., R. Kumar, …, D. K. Klimov. 2010. Nonsteroidal anti-inflammatory drug naproxen destabilizes Aβ amyloid fibrils: a molecular dynamics investigation. *J. Phys. Chem. B.* 114:15394–15402.
36. Brooks, B. R., R. E. Bruccoler, …, M. Karplus. 1982. CHARMM: a program for macromolecular energy, minimization, and dynamics calculations. *J. Comput. Chem.* 4:187–217.
37. Ferrara, P., J. Apostolakis, and A. Caflisch. 2002. Evaluation of a fast implicit solvent model for molecular dynamics simulations. *Proteins.* 46:24–33.
38. Takeda, T., and D. K. Klimov. 2009. Probing energetics of Abeta fibril elongation by molecular dynamics simulations. *Biophys. J.* 96:4428–4437.
39. Hou, L., H. Shao, …, M. G. Zagorski. 2004. Solution NMR studies of the Aβ(1-40) and Aβ(1-42) peptides establish that the Met35 oxidation state affects the mechanism of amyloid formation. *J. Am. Chem. Soc.* 126:1992–2005.
40. Takeda, T., and D. K. Klimov. 2009. Probing the effect of amino-terminal truncation for Abeta1-40 peptides. *J. Phys. Chem. B.* 113:6692–6702.
41. Thomas, T., T. G. Nadackal, and K. Thomas. 2001. Aspirin and non-steroidal anti-inflammatory drugs inhibit amyloid-β aggregation. *Neuroreport.* 12:3263–3267.
42. Sugita, Y., and Y. Okamoto. 1999. Replica-exchange molecular dynamics method for protein folding. *Chem. Phys. Lett.* 114:141–151.
43. Chang, W. E., T. Takeda, …, D. K. Klimov. 2010. Molecular dynamics simulations of anti-aggregation effect of ibuprofen. *Biophys. J.* 98: 2662–2670.
44. Kabsch, W., and C. Sander. 1983. Dictionary of protein secondary structure: pattern recognition of hydrogen-bonded and geometrical features. *Biopolymers.* 22:2577–2637.
45. Kim, S., T. Takeda, and D. K. Klimov. 2010. Mapping conformational ensembles of aβ oligomers in molecular dynamics simulations. *Biophys. J.* 99:1949–1958.
46. Ferrenberg, A. M., and R. H. Swendsen. 1989. Optimized Monte Carlo data analysis. *Phys. Rev. Lett.* 63:1195–1198.
47. Morris, G. M., R. Huey, …, A. J. Olson. 2009. AutoDock4 and AutoDockTools4: Automated docking with selective receptor flexibility. *J. Comput. Chem.* 30:2785–2791.
48. Petkova, A. T., W.-M. Yau, and R. Tycko. 2006. Experimental constraints on quaternary structure in Alzheimer's β-amyloid fibrils. *Biochemistry.* 45:498–512.
49. Kim, S., T. Takeda, and D. K. Klimov. 2010. Globular state in the oligomers formed by Abeta peptides. *J. Chem. Phys.* 132:225101.
50. Convertino, M., R. Pellarin, …, A. Caflisch. 2009. 9,10-Anthraquinone hinders β-aggregation: how does a small molecule interfere with Abeta-peptide amyloid fibrillation? *Protein Sci.* 18:792–800.
51. Raman, E. P., T. Takeda, and D. K. Klimov. 2009. Molecular dynamics simulations of Ibuprofen binding to Abeta peptides. *Biophys. J.* 97: 2070–2079.
52. Wu, C., M. Biancalana, …, J. E. Shea. 2009. Binding modes of thioflavin-T to the single-layer β-sheet of the peptide self-assembly mimics. *J. Mol. Biol.* 394:627–633.
53. Yang, F., G. P. Lim, …, G. M. Cole. 2005. Curcumin inhibits formation of amyloid beta oligomers and fibrils, binds plaques, and reduces amyloid in vivo. *J. Biol. Chem.* 280:5892–5901.
54. Chen, J., A. H. Armstrong, …, M. H. Hecht. 2010. Small molecule microarrays enable the discovery of compounds that bind the Alzheimer's Aβ peptide and reduce its cytotoxicity. *J. Am. Chem. Soc.* 132:17015–17022.